GateCT™ surface tracking system for respiratory signal reconstruction in 4DCT imaging

Kevin I. Kauweloa
Department of Physics, San Diego State University, San Diego, California 92182 and Center for Advanced Radiotherapy Technologies and Department of Radiation Medicine and Applied Sciences, University of California San Diego, La Jolla, California 92093

Dan Ruan
Department of Radiation Oncology, University of California Los Angeles, Los Angeles, California 90095

Justin C. Park, Ajay Sandhu, Gwe Ya Kim, Todd Pawlicki, W. Tyler Watkins, and Bongyong Song
Center for Advanced Radiotherapy Technologies and Department of Radiation Medicine and Applied Sciences, University of California San Diego, La Jolla, California 92093

William Y. Song[a)]
Center for Advanced Radiotherapy Technologies and Department of Radiation Medicine and Applied Sciences, University of California San Diego, La Jolla, California 92093

(Received 28 July 2011; revised 6 November 2011; accepted for publication 5 December 2011; published 30 December 2011)

Purpose: To assess the temporal and spatial accuracy of the GateCT™ system (VisionRT, London, UK), a recently released respiratory tracking system for 4DCT, under both ideal and nonideal respiratory conditions.
Methods: Three experiments were performed by benchmarking and comparing its results with the ground-truth input data and those generated by the widely used Varian RPM™ system (Real-time Position Management, Varian, Palo Alto, CA). The first experiment used 10 sinusoidal breathing patterns (constant amplitude and frequency using $\sin^6\omega t$), 10 "consistent" patient breathing patterns, and 10 "sporadic" patient breathing patterns. Motion was simulated with the QUASAR™ Programmable Respiratory Motion Platform (MODUS, London, Canada) as the surrogate. The GateCT™ and RPM™ systems were used to track the breathing patterns. The data from both systems were then analyzed in the Fourier domain, to evaluate temporal/phase accuracy, using the Pearson's correlation coefficient (PCC). The analysis correlated the ground-truth input data against the GateCT™ and RPM™ tracking results, respectively. The second experiment used 10 ideal sinusoidal breathing patterns, five of period 2.0 s, and five of period 5.0 s, with varying abdominal amplitudes found in clinical cases (peak-to-peak range: 1.67–10 mm) to test the sensitivity of the system to reconstruct various range of motion. And, the third experiment used 12 consecutive clinical patients to track the abdominal motion simultaneously by the GateCT™ and RPM™ systems. The baseline of the tracking results from both the two systems was analyzed via the mean-position-estimate (MPE) calculations. All experiments were tracked for at least 120 s.
Results: In the first experiment, the average PCC values ($\pm$SD) of all thirty breathing patterns were 0.9995 ± 0.00035 and 0.9994 ± 0.00041 for the GateCT™ and the RPM™ system, respectively. These nearly identical results demonstrated similar temporal/phase tracking accuracy for the two systems. The results in the second experiment, however, revealed a pattern for the GateCT™ system in which the uncertainty of its mean-position tracking increased as the amplitude of the breathing pattern decreased. For example, a non-negligible baseline drift of up to 29.3% with respect to the peak-to-peak amplitude of 1.67-mm was observed. On the contrary, the RPM™ system displayed a more consistent recording of amplitudes over time with the greatest drift being $<7.7\%$. The third experiment confirmed these findings in the clinical setting. Consistent decrease in PCC values due to the increase in artificial amplitude drifts, as the breathing amplitude decreased, was found. The lowest PCC value was 0.7239 for a patient with 1.57-mm peak-to-peak amplitude.
Conclusions: The GateCT™ system revealed its consistency in temporal/phase tracking but had limitations in accurately tracking the absolute abdominal positions, thus suggesting its appropriateness for phase-sorting of 4DCT rather than amplitude-sorting. In contrast, the RPM™ system demonstrated stable respiratory signal tracking in all ranges and accurately both in phase and amplitude, and is a robust system to use for both phase-sorting and amplitude-sorting techniques. The impact of the observed mean-position drift in the GateCT™ system on the resulting 4DCT image quality, in amplitude-sorting, needs further investigation. [DOI: 10.1118/1.3671941]

Key words: GateCT, RPM, 4DCT, commissioning, respiratory tracking

I. INTRODUCTION

Moving tumors (lung, liver cancer, etc.) complicate both treatment planning and dose delivery when compared to static tumors.[1–7] Four-dimensional computed tomography (4DCT) has significantly alleviated the difficulties presented with moving tumors by organizing CT projections to successfully capture motion.[1–6] There are two ways in which 4DCT organizes its data: (1) phase-based sorting and (2) amplitude-based sorting.[2,5–7] Phase-based sorting combines CT projections acquired during each specific phase within the patient's breathing pattern, while amplitude-based sorting combines all CT projections acquired when the tumor's position falls within a specific amplitude bin.[2,5,6] In order to successfully reconstruct an image free of motion artifacts, the tracking system must accurately record the patient's breathing pattern so the CT projections are correctly sorted. This is a significant challenge in 4DCT.[2,5–8]

Many respiratory tracking tools have been developed to accomplish the goal of producing high-quality 4DCT images,[1–7,9] but like all tools, flaws may exist and thus need to be evaluated before clinical application. Otani *et al.*,[7] for example, studied the difference between two different respiratory tracking tools: AZ-733V™ (Anzai Medical, Shinagawa, Tokyo) and RPM™ (Real-time Position Management, Varian, Palo Alto, CA). They observed a large phase difference between the recordings of each system due to irregularity of patient breathing and thus concluded that the phase difference of irregular breathing between the two systems were due to the different algorithms each system used. They also concluded that the observed phase differences can lead to inaccurate estimations of the internal target volume (ITV) which may result in the failure of radiation treatment.

Similar to the Otani *et al.*[7] study, this paper focuses on the evaluation of the GateCT™ system (VisionRT, London, UK). Two respiratory tracking tools observed in this study are installed at the Moores Cancer Center, University of California San Diego: the RPM™ system and the recently released GateCT™ system. With three different experiments, we tested the temporal/phase and spatial accuracy of the GateCT™ system by benchmarking and comparing its results to the input ground-truth data as well as the data of the RPM™ system. Following the acquisition of the tracking results from these two systems, the first experiment evaluated its temporal/phase accuracy while the second and third experiments evaluated its spatial accuracy in terms of amplitude detection. If temporal synchronization does not exist between the patient's breathing pattern and the tracking results of a system, inaccurate phase-sorting will be present. On the other hand, if the tracking system incorrectly positions the patient's abdominal surface, then inaccurate amplitude-sorting will be present. The bottom line is, if either inaccurate phase-based or amplitude-based sorting exists, significant motion artifacts will appear in the reconstructed 4DCT image which will compromise the radiation treatment. The current study is focused on examining the accuracy of the respiratory signals tracked by the GateCT™ system only. Thus, the subsequent impact of its accuracy on 4DCT image quality is left as a follow-up study.

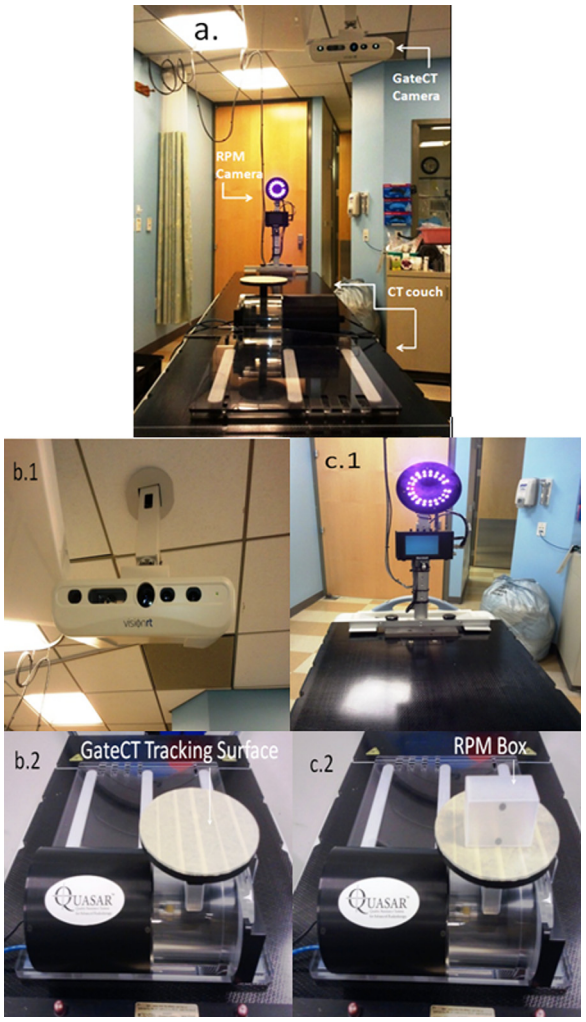

FIG. 1. (a) The experimental setup with the components listed. (b.1) The GateCT™ camera, (b.2) the round GateCT™ tracking surface of the QUASAR phantom, (c.1) the RPM™ camera, and (c.2) the RPM™ box placed on the QUASAR phantom.

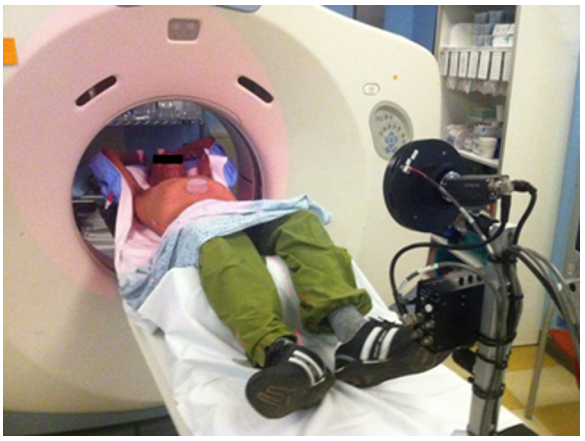

FIG. 2. A clinical 4DCT simulation patient setup for Experiment 3. The GateCT™ and RPM™ simultaneously tracked the patients' abdomen. The large elliptical-shaped red light is used by the GateCT™ system to create a patient topology, for tracking purposes.

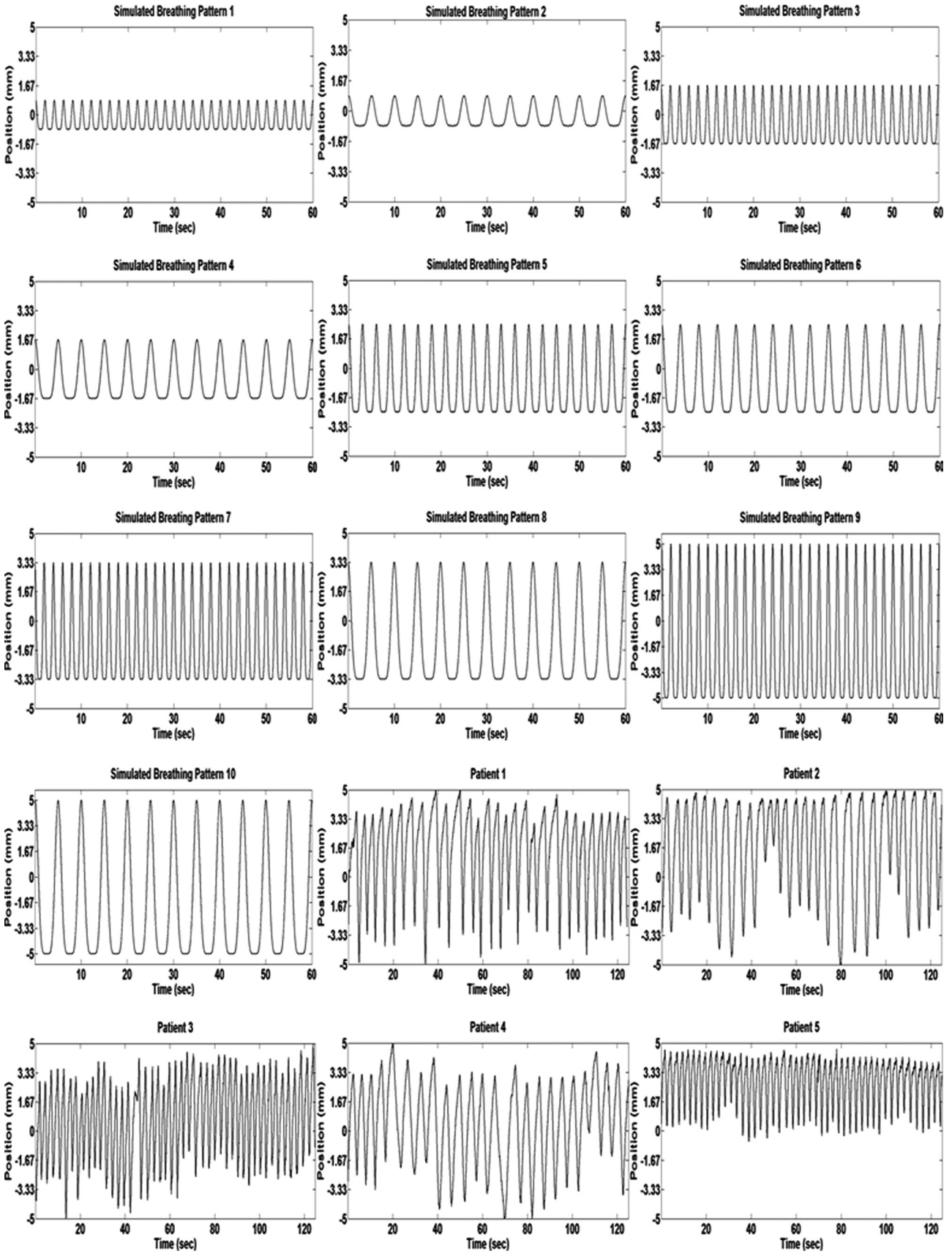

FIG. 3. The 30 respiratory patterns studied in Experiment 1: 10 simulated sinusoidal patterns, 10 regular patient breathing patterns, and 10 irregular patient breathing patterns.

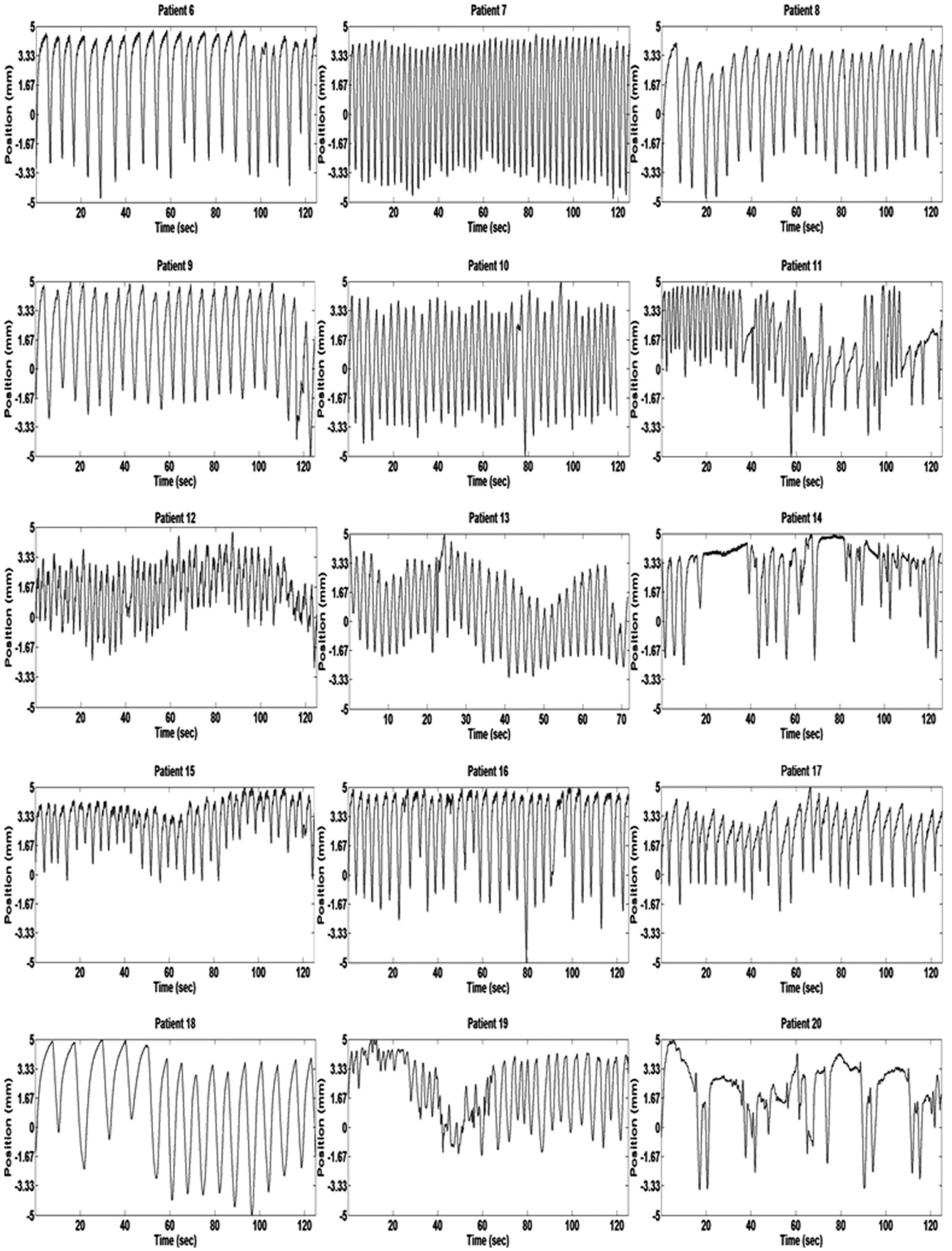

FIG. 3. (*Continued*)

II. METHODS AND MATERIALS

The GateCT™ respiratory tracking system for 4DCT applications is based on the design of the AlignRT™ system (VisionRT, London, UK), originally used for patient setup assessment.[10–12] The GateCT™ system uses a single camera mounted on the ceiling above the foot of the couch, as shown in Fig. 1, for markerless patient surface tracking, and generates surface data at a 15 Hz frame rate. The RPM™ system uses a single camera fixed to the foot of the CT couch and has a constant sampling frequency of 30 Hz. Figure 1 shows the GateCT™ system (v2.3), the RPM™ system (v1.7), and the experimental setup.

The QUASAR Programmable Respiratory Motion Platform (QPRMP) (MODUS, London, Canada) is used to simulate a prespecified, input respiratory waveform. Figure 1(a) shows the QPRMP and the components used for this study. This experiment utilized the circular platform, which moves in the vertical direction, for pseudo-abdominal motion simulation. The patient respiratory patterns were provided by the software of QUASAR and the sinusoidal "$\sin^6\omega t$" patterns were generated using MATLAB 2010a (MathWorks, Natick, MA). For the experiment involving real patients, Fig. 2 illustrates the setup. All respiratory patterns were tracked for at least 120 s.

II.A. Experiment 1: Temporal accuracy

This experiment was designed to test the temporal accuracy of the input signals. The QPRMP plate moved in accordance to the specific input breathing pattern being studied. As shown in Fig. 3, and listed in Table I, this experiment involved ten simulated "$\sin^6\omega t$" sinusoidal patterns, ten consistent patient breathing patterns, and ten sporadic

TABLE I. List of PCC calculations for the 30 respiratory signals analyzed. Also listed are the peak-to-peak amplitudes and periods of each signal evaluated.

Sinusoidal breathing patterns (SBP)				
Breathing pattern	Amplitude (mm)	Period (s)	PCC[a]: GCT vs SBP	PCC: RPM vs SBP
1	1.67	2.00	0.9982	0.9992
2	1.67	5.00	0.9992	0.9986
3	3.33	2.00	0.9999	0.9999
4	3.33	5.00	0.9992	0.9997
5	5.00	3.00	0.9995	0.9994
6	5.00	4.00	0.9995	0.9996
7	6.67	2.00	0.9995	0.9996
8	6.67	5.00	0.9996	0.9993
9	10.0	2.00	0.9998	0.9997
10	10.0	5.00	0.9997	0.9996
Good patient breathing patterns				
Patient	Amplitude (mm)	Period (s)	GCT vs patient	RPM vs patient
1	7.550 ± 0.884	4.269 ± 0.719	0.9995	0.9999
2	7.020 ± 1.710	4.595 ± 0.812	0.9999	0.9998
3	6.270 ± 1.181	2.645 ± 0.237	0.9995	0.9997
4	6.636 ± 1.113	5.359 ± 1.047	0.9997	0.9995
5	4.076 ± 0.449	2.654 ± 0.187	0.9992	0.9998
6	7.482 ± 0.835	5.514 ± 0.992	0.9997	0.9998
7	7.769 ± 0.596	2.697 ± 0.197	0.9996	0.9986
8	6.513 ± 0.739	4.788 ± 0.579	0.9999	0.9998
9	6.687 ± 0.666	5.351 ± 0.404	0.9989	0.9983
10	6.799 ± 0.843	3.253 ± 0.375	0.9998	0.9994
Bad patient breathing patterns				
Patient	Amplitude (mm)	Period (s)	GCT vs patient	RPM vs patient
11	4.755 ± 1.375	3.033 ± 1.264	0.9995	0.9998
12	3.655 ± 0.864	2.704 ± 0.260	0.9998	0.9999
13	4.618 ± 0.797	1.925 ± 0.208	0.9994	0.9988
14	3.432 ± 2.168	4.613 ± 3.988	0.9996	0.9999
15	3.143 ± 0.858	3.534 ± 0.472	0.9997	0.9999
16	6.153 ± 1.212	4.106 ± 0.743	0.9997	0.9997
17	4.442 ± 0.743	4.350 ± 0.669	0.9998	0.9999
18	6.871 ± 1.167	8.477 ± 1.814	0.9992	0.9998
19	2.707 ± 1.555	3.417 ± 1.109	0.9998	0.9999
20	3.412 ± 2.006	5.925 ± 5.333	0.9996	0.9977

[a]PCC ≡ Pearson's correlation coefficient.

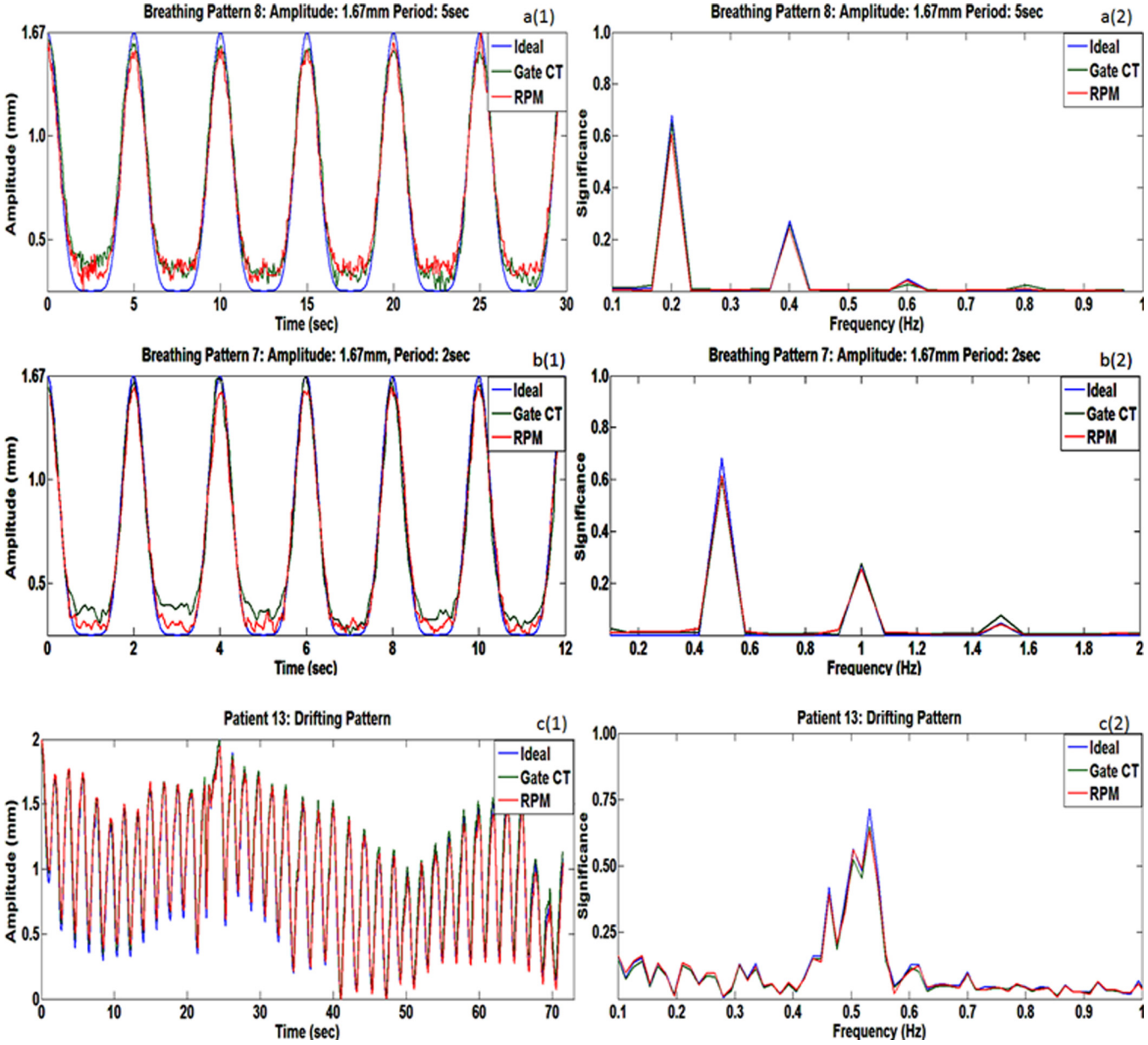

FIG. 4. Three sample signals from the 30 tested patterns with spatial representation on the left and frequency representation on the right.

patient breathing patterns. These thirty traces were used as input to the QPRMP, and are considered as the ground-truth.

Due to the subjective, manual overlapping of the traces from both systems for data analysis, there is a small error in positioning. In order to avoid the recorded spatial positioning from influencing the calculations of temporal accuracy, the Fourier[14] transform was applied. Fourier transform is a mathematical technique which reveals the different frequencies (e.g., temporal frequency) of a wave of interest that, when put into sine and cosine functions and summed, will produce the original wave. If two waves of the same frequency are out of phase and the Fourier transform is applied to each, the frequencies of both waves will be shown to be equal in the frequency domain. Having the accuracy analysis in the frequency domain renders it free from the uncertainties in the manual matching of the traces and from amplitude variations in signals.

The Fourier transform was applied to all thirty tracked traces. They were then juxtaposed in the frequency domain (for example in Fig. 4) and compared using the Pearson product-moment correlation coefficient (PCC), defined as[13,14]

TABLE II. Summary of the information listed in Table I.

System	Breathing pattern group	Avg. PCC	SD[a] of PCC	RSE[a]
GateCT™	Simulated	0.9994	±0.0004818	0.0482%
	Good	0.9996	±0.0003164	0.0317%
	Bad	0.9996	±0.0001969	0.0197%
	All breathing patterns	0.9995	±0.0003505	0.0351%
RPM™	Simulated	0.9993	±0.0005587	0.0559%
	Good	0.9995	±0.0005582	0.0558%
	Bad	0.9995	±0.0007258	0.0726%
	All breathing patterns	0.9994	±0.0006048	0.0605%

[a]RSE ≡ Relative standard error, SD ≡ Standard deviation.

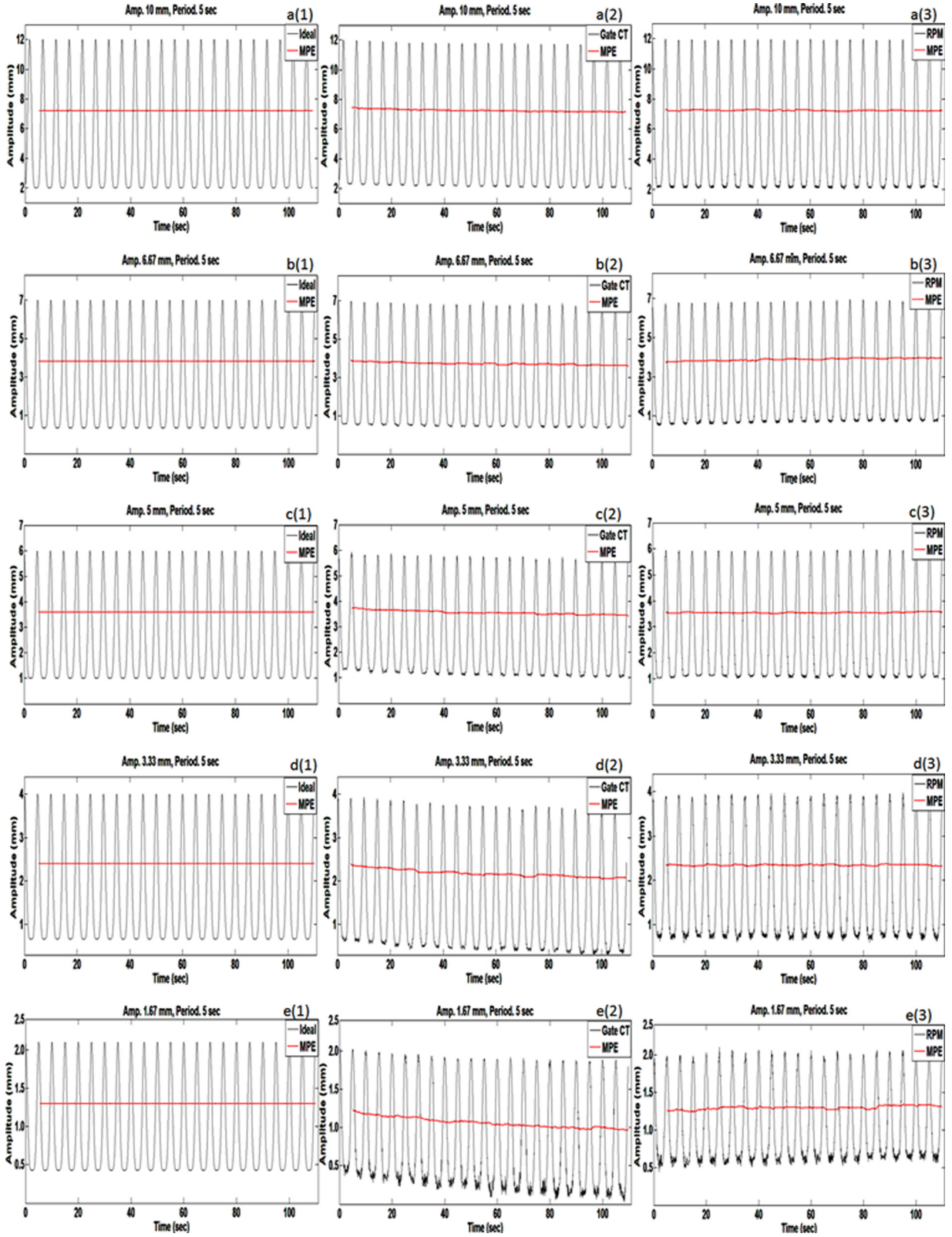

FIG. 5. Five sinusoidal patterns with decreasing amplitudes from 10 to 1.67 mm, with a constant period of 5.0 s. Each column represents the ground-truth (left), GateCT™ (center), and RPM™ (right) data.

$$\mathrm{PCC} = \frac{1}{n-1}\sum_{i=1}^{n}\left(\frac{A_i - \bar{A}}{s_A}\right)\left(\frac{B_i - \bar{B}}{s_B}\right), \tag{1}$$

where $\bar{A}$ and $\bar{B}$ are the sample mean from the tracking record and input trace, respectively, s_A and s_B are the corresponding standard deviations, and n is the number of data points. This empirical correlation quantitatively measures the similarity between the tracking results and ground-truth data. The PCC value ranges from -1 to 1 with 1 being exact correlation, -1 being exactly opposite correlation and 0 implying no

similarity between signals.[12,13] This analysis was performed on both the GateCT™ and RPM™ data. It should be pointed out that due to the phase-based sorting technique being one major method of projection rebinning for 4DCT reconstruction, the frequencies of the tracked traces are very important. If the tracking system records inaccurate frequencies, then incorrect rebinning will result in rendering of image artifacts that are highly undesired.

II.B. Experiment 2: Spatial accuracy

This experiment was designed to test the spatial accuracy of the generated signals. We used 10 simulated "$\sin^6\omega t$" sinusoidal patterns, five of period 2.0 s and five of period 5.0 s, with varying abdominal amplitudes found in clinic (peak-to-peak range: 1.67–10 mm). The experimental setup was the same as in Experiment 1. To analyze the spatial accuracy, the baseline of the signals was calculated [i.e., mean-position-estimate (MPE)]. The MPE is used due to its capability of revealing a quantitative significance of the artificial drift present in the tracked signals. The MPE for all three data sets (i.e., input, GateCT™, and RPM™) were then compared to determine the spatial accuracy of each system's signal.

The running mean-position is estimated by an ellipse-fitting[8,16–20] based approach. The key idea is to consider the observed position values as projections of noisy samples from an underlying ellipse undergoing slow temporal evolution. Algorithmic-wise, the samples within a sliding temporal window is first augmented by state lagging to a 2D space $\{x_i = s(t_i), y_i = x_{i-1}\}$. The samples (x_i,y_i) then manifests into points on the elliptical boundary. The elliptical-fitting method is then applied by fitting the collection of points (x_i, y_i), $i = 1,2,\ldots K$ where K is the total number of samples within the sliding window for the specific time instant, to the elliptical equation[7]

$$ax^2 + bxy + cy^2 + dx + ey + f = 0, \tag{2}$$

subject to $(b^2 - 4ac) < 0$. Once the coefficients of Eq. (2) are determined, the center point, which creates the MPE line, is calculated with

$$x_o = \frac{2cd - bf}{b^2 - 4ac}, \quad y_o = \frac{2af - bd}{b^2 - 4ac}. \tag{3}$$

TABLE III. The magnitudes of baseline drift observed in Experiment 2.

System	Breathing amplitude (mm)	Magnitude drift percentage (%)
Gate CT™	10.0	6.53
	6.67	9.17
	5.00	14.05
	3.33	20.13
	1.67	29.31
RPM™	10.0	0.593
	6.67	7.74
	5.00	0.853
	3.33	0.706
	1.67	5.76

TABLE IV. PCC values calculated between the RPM™ and the GateCT™ traces, using the MPE values, in Experiment 3. The list is in descending order of the breathing amplitudes.

Patient No.	Patient breathing period (s)	Patient breathing amplitude (mm)	PCC of each MPE
1	4.942 ± 0.346	19.08 ± 1.870	0.9357
2	8.709 ± 0.397	18.51 ± 1.320	0.9483
3	6.770 ± 0.962	15.72 ± 2.770	0.9771
4	2.963 ± 0.309	11.43 ± 2.470	0.8594
5	8.934 ± 0.882	9.969 ± 1.230	0.8399
6	3.699 ± 0.337	7.321 ± 0.938	0.9853
7	4.261 ± 0.501	5.995 ± 0.958	0.8478
8	5.878 ± 0.833	5.922 ± 0.731	0.8259
9	3.470 ± 0.225	5.791 ± 0.496	0.8618
10	3.615 ± 0.535	3.867 ± 0.408	0.8746
11	2.341 ± 0.162	1.792 ± 0.219	0.7835
12	1.963 ± 0.131	1.574 ± 0.334	0.7239

The ellipse center is then projected back into the 1D space where the original data were acquired in. Repeating this procedure for every sliding window yields a running mean-position trajectory for the semi-periodic respiratory trajectory.

II.C. Experiment 3: Spatial accuracy of clinical patient cases

This experiment was performed to confirm the results of Experiment 2 (i.e., significant amplitude drift of GateCT™ traces) on actual clinical setup. Twelve patients were consecutively analyzed. Each patient was placed on the CT couch using a wing-board and an upper vac lok, as shown in Fig. 2. Once the patient setup was completed, the tracking point for the GateCT™ system was set. The point was deliberately chosen to be directly below (nearest possible) the RPM box such to guarantee the equality of the input motion. MPE analysis, similar to that in Experiment 2, was performed on all traces. All experiments were tracked for at least 120 s.

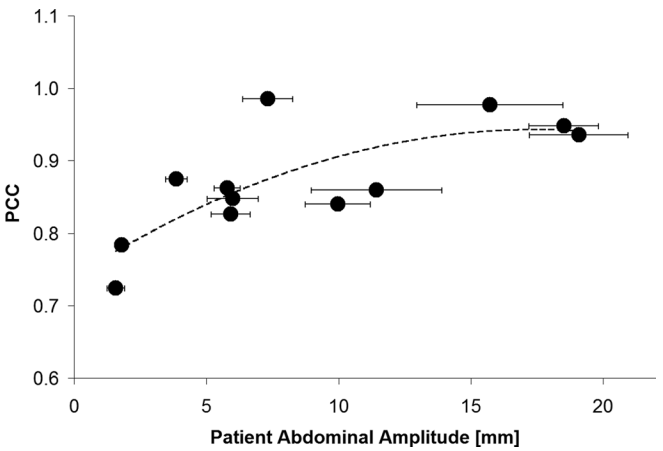

FIG. 6. Plot of Table IV illustrating the dependence of the PCC value to the breathing amplitude. A second-power polynomial function was fit to the plot.

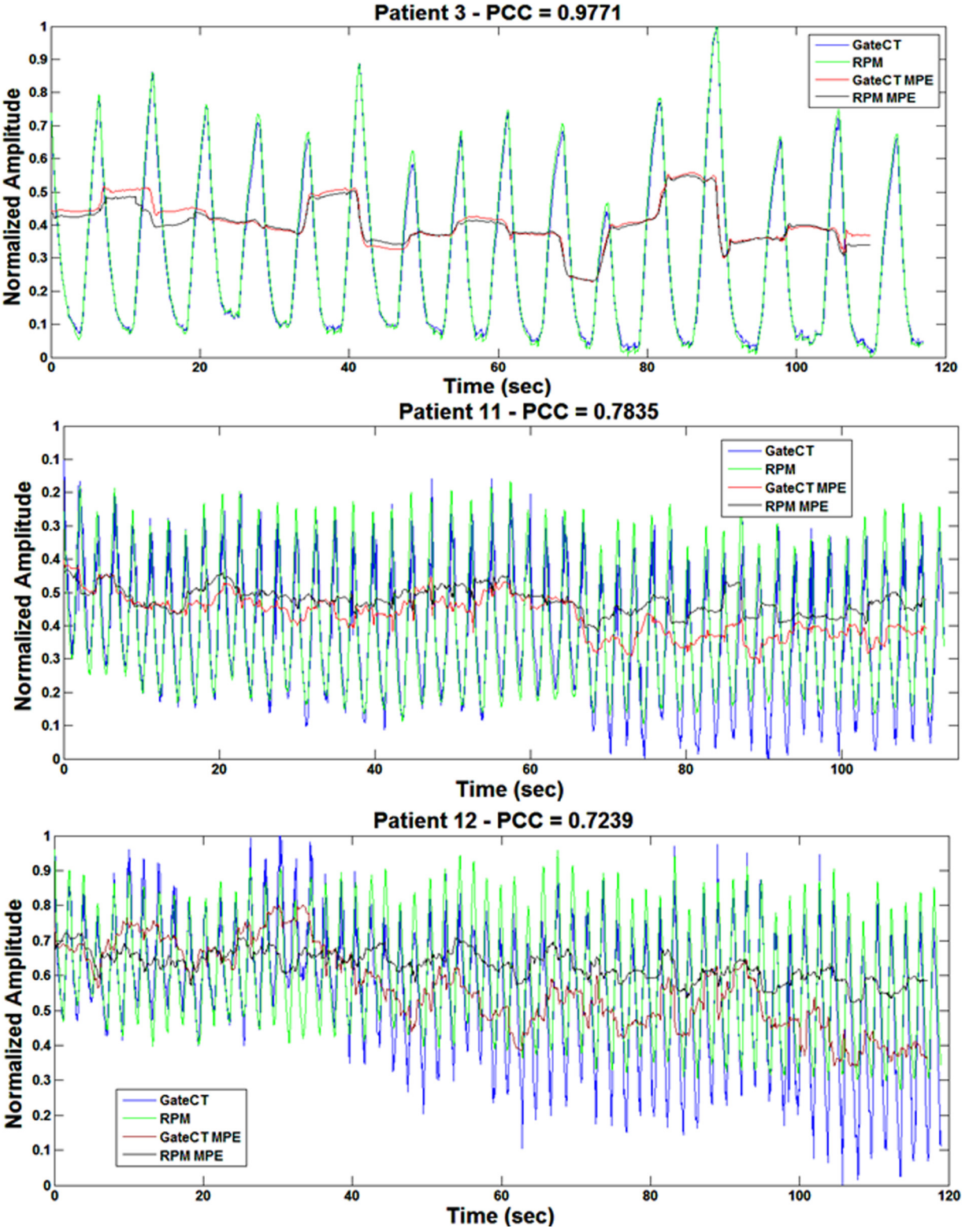

FIG. 7. Three selected breathing traces for illustrating the cases with both no drift and artificial drift of the GateCT™ traces listed in Table IV.

III. RESULTS

III.A. Experiment 1: Temporal accuracy

Tables I and II list the relationships between the ground-truth respiratory patterns and both the GateCT™ and RPM™ recorded data with PCC analyses. Both systems provided >0.999 average PCC correlations, for sinusoidal, consistent, and sporadic patient breathing patterns. The lowest PCC correlation of the 30 patterns was found to be 0.9982 (Breathing Pattern 1) with GateCT™ and 0.9977 (Patient 20) with RPM™. Out of all GateCT™ recorded breathing patterns, >98% of them had a PCC correlation of

0.9986 or higher. Similar results held for the RPM^{TM} system also.

Figure 4 displays the temporal and Fourier domain signals of three representative samples from the thirty patterns in Table I. The results in the Fourier domain display and confirm the strong correlation between the GateCT^{TM}, RPM^{TM}, and ground-truth data.

III.B. Experiment 2: Spatial accuracy

Figure 5 displays five sinusoidal patterns with decreasing amplitudes from 10 to 1.67 mm, with a constant period of 5.0 s. Each column represents the ground-truth (left), GateCT^{TM} (center), and RPM^{TM} (right) data. The GateCT^{TM} system's tracking results showed increasing baseline drifts as the amplitude of the respiratory signal decreased. Since the ground-truth signals are ideal sinusoidal patterns with no drifts, the drift is caused solely by the GateCT^{TM} system. The experiment had been repeated numerous times to verify the consistency of this behavior and rendered similar results.

Table III lists the quantitative values of the drifts. For the GateCT^{TM}, an upward of ~30% drift relative to the input peak-to-peak amplitude was found (i.e., for peak-to-peak amplitude of 1.67 mm). For the RPM^{TM} system, there were some observed drifts, similar to that found in the GateCT^{TM} system, of up to 7.74% in 6.67-mm amplitude. However, there was no noticeable trend or relationship with the input amplitude magnitude and the MPE errors were mostly smaller than those of the GateCT^{TM}.

III.C. Experiment 3: Spatial accuracy of clinical patient cases

Table IV lists the PCC values calculated between the RPM^{TM} and the GateCT^{TM} traces, for each of the 12 patients. It was observed that, in Fig. 6, as the amplitude of the breathing decreased, there was a gradual and clear pattern of decrease in the PCC values.

Figure 7 shows three selected breathing traces for illustration. As can be seen, for an amplitude that is well above 2 mm (Patient 3, 15.72 ± 2.770 mm), there is no drift in the GateCT^{TM} trace, whereas the drift becomes noticeable for the two cases with <2 mm amplitude, as in Patients 11 and 12.

IV. DISCUSSION

The GateCT^{TM} system varied in its accuracy in terms of phase and amplitude tracking of respiratory signals. Experiment 1 confirmed the GateCT^{TM} system's accuracy in phase tracking, while Experiments 2 and 3 revealed its limitations in accurately recording the absolute position of the tracking surface, especially for smaller amplitudes (≤ 2 mm), as shown in Figs. 5–7. It is important to note that the amplitude drift of the GateCT^{TM} system is independent of the breathing period, as shown in Experiment 2. These findings allude to the utility of using the GateCT^{TM} system for phase-sorting to obtain high-quality 4DCT images, and caution against its use in amplitude-sorting due to the artificial drifts.

In all three experiments, the RPM^{TM} system tracked both the phase and amplitude of the input signals accurately. This is comforting to know since the system has been in clinical use for a long time. However, it requires placing an RPM block and adjusting the RPM camera for each scan, while the GateCT^{TM} system is more convenient and easy to use as there are no physical parts to setup/move. In addition, the current GE CT systems used at our clinic only provide the option for phase-based projection sorting. These practical considerations make the GateCT^{TM} system a decent, alternative option for respiratory signal generation of 4DCT simulations. In addition, it is hoped that the near-future versions of GateCT^{TM} may have this baseline drift problem fixed (the current version we tested was v2.3), as we have contacted the VisionRT company of this artificial drift issue. At current, the reason for such a drift has not been resolved, however.

This work has laid out a practical procedure to test and evaluate a new respiratory tracking system for 4DCT simulation. The analysis of the resulting image quality and its impact on radiation treatment planning in terms of accurate ITV generations, from respiratory signal recordings generated by both the GateCT^{TM} and RPM^{TM} systems, are planned in a follow-up study.

V. CONCLUSIONS

The GateCT^{TM} system revealed its consistency in phase tracking but had limitations in accurately tracking the absolute surface positions of low amplitudes, thus suggesting its appropriateness for phase-sorting of 4DCT projections rather than amplitude-sorting. In contrast, the RPM^{TM} system demonstrated stable respiratory signal tracking in all ranges and accurately both in phase and amplitude and is a robust system to use for both phase- and amplitude-sorting techniques. The impact of the observed mean-position drift in the GateCT^{TM} system on the resulting 4DCT image quality, in amplitude-sorting, needs further investigation.

ACKNOWLEDGMENTS

W.Y.S. acknowledges that this project is partially supported by the Clinical & Translational Research Institute 2011 Pilot Innovative Technology Grant provided through the University of California San Diego. Dr. Pawlicki acknowledges travel support and honoraria from VisionRT. There are no conflicts of interest for the remaining authors.

[a]Author to whom correspondence should be addressed. Electronic mail: wysong@ucsd.edu. Telephone: (858) 246-0886; Fax: (858) 822-5568.

[1]S. S. Vedam, P. J. Keall, V. R. Kini, H. Mostafavi, H. P. Shukla, and R. Mohan, "Acquiring a four-dimensional computed tomography dataset using an external respiratory signal," Phys. Med. Biol. **48**(1), 45–62 (2003).

[2]W. Lu, P. J. Parikh, J. P. Hubenschmidt, J. D. Bradley, and D. A. Low, "A comparison between amplitude sorting and phase angle sorting using external respiratory measurement for 4DCT," Med. Phys. **33**(8), 2964–2974 (2006).

[3]P. Keall, "4-Dimensional computed tomography imaging and treatment planning," Semin. Radiat. Oncol. **14**(1), 81–90 (2004).

[4]D. A. Low, M. Nystrom, F. Kalinin, and P. Parikh, "A method for the reconstruction of four-dimensional synchronized CT scans acquired during free breathing," Med. Phys. **30**(6), 1254–1263 (2003).

[5]M. J. Fitzpatrick, G. Starkschall, and J. A. Antolak, "Displacement-based binning of time-dependent computed tomography image data sets," Med. Phys. **33**(1), 235–246 (2006).
[6]N. M. Wink, C. Panknin, and T. D. Soldberg, "Phase versus amplitude sorting of 4D-CT data," J. Appl. Clin. Med. Phys. **7**(1), 77–85 (2006).
[7]Y. Otani, T. Teshima, I Fukuda, N tsukamoto, Y Kumazaki, H Sekine, T Dokiya, E Imabayashi, O Kawaguchi, and T Nose, "A comparison of the respiratory signals acquired by different respiratory monitoring systems used in respiratory gated radiotherapy," Med. Phys. **37**(12), 6178–6186 (2010).
[8]D. Ruan, J. A. Fessler, and J. M. Balter, "Mean position tracking of respiratory motion," Med. Phys. **35**(2), 782–792 (2008).
[9]V. R. Kini, S. S. Vedam, P. J. Keall, S. Patil, C. Chen, and R. Mohan, "Patient training in respiratory-gated radiotherapy," Med. Dosim. **28**(1), 7–11 (2003).
[10]M. F. Spadea, G. Baroni, D. P. Gierga, J. C. Turcotte, D. P. Gierga, G. T. Y. Chen, and G. C. Sharp, "Evaluation and commissioning of a surface based system for respiratory sensing in 4D CT," J. Appl. Clin. Med. Phys. **12**(1), 162–169 (2011).
[11]C. Bert, K. G. Metheany, K. Doppke, and G. T. Y. Chen, "A phantom evaluation of a stereo-vision surface imaging system for radiotherapy patient setup," Med. Phys. **32**(9), 2753–2762 (2005).
[12]M. Krengli, S. Gaiano, E. Mones, A. Ballare, D. Beldi, C. Bolchini, and G. Loi, "Reproducibility of patient setup by surface image registration system in conformal radiotherapy of prostate cancer," Radiother. Oncol. **4**, 9 (2009).
[13]A. Buda and A. Jarynowski, *Life-Time of Correlations and Its Applications (Vol 1)* (Wydawnictwo. Niezalezne, 2010), pp. 5–21.
[14]J. Cohen, *Statistical Power Analysis for the Behavioral Sciences*, 2nd ed. (Lawrence Erlbaum Associates, Inc., New Jersey, 1988).
[15]R. N. Bracewell, *The Fourier Transform and Its Applications*, 3rd ed. (McGraw-Hill, Boston, 2000).
[16]A. Fitzgibbon, M. Pilu, and R. B. Fisher, "Direct least square fitting of ellipses," IEEE. Trans. Pattern Anal. Mach. Intell. **21**, 476–480 (1999).
[17]D. Ruan and J. A. Fessler, "Adaptive ellipse tracking and a convergence proof," Technical Report No. 382. (Comm. And Sign. Proc. Lab., Dept of EECS, University of Michigan, Ann Arbor, MI, 2007).
[18]D. Ruan, J. A. Fessler, J. M. Balter, and P. J. Keall, "Real-time profiling of respiratory motion: baseline drift, frequency variation, and fundamental pattern change," Phys. Med. Biol. **54**(15), 4777–4792 (2009).
[19]E. S. Maini, "Enhanced direct least square fitting of ellipses," Int. J. Pattern Recognit. Artif. Intell. **20**(6), 939–953 (2006).
[20]R. Halir and J. Flusser, "Numerically stable direct least squares fitting of ellipses," *Proceedings of WSCG* (1998).